The Synthesis of Alginate-Capped Silver Nanoparticles under Microwave Irradiation

Foliatini[1,2], Yoki Yulizar[1] & Mas Ayu Elita Hafizah[3]

[1]Department of Chemistry, Faculty of Mathematics and Natural Sciences, Universitas Indonesia, Kampus UI Depok 16424, Indonesia
[2]Bogor AKA Polytechnic, Jl. Pangeran Sogiri No. 283 Tanah Baru, Bogor 16158, Indonesia
[3]Postgraduate Program of Material Science, Faculty of Mathematics and Natural Sciences, Universitas Indonesia, Jl. Salemba Raya No. 4, Jakarta 16440, Indonesia
Email: yokiy@ui.ac.id

Abstract. Synthesis of silver nanoparticles (Ag-NP) was successfully performed within a few minutes by microwave irradiation of the precursor salt ($AgNO_3$) and alginate mixed solution in one pot. Herein, alginate molecules acted as both a reducing and stabilizing agent for the preparation of the silver nanoparticles. The obtained nanoparticles were characterized by ultraviolet-visible (UV-Vis) spectroscopy, particle size analysis (PSA), Fourier transform infrared spectroscopy (FTIR), and transmission electron microscopy (TEM). The pH and concentration ratio of the alginate/metal precursor salt greatly influenced the particle size and its distribution of Ag-NP. The higher the pH the higher the nucleation rate and the larger the electrostatic stabilization, while both of them were responsible for producing a smaller particle size and a narrower size distribution. A higher concentration ratio also yielded a smaller particle size and a narrower size distribution, but above the optimum ratio, the trend was conversely changed due to the reducing capability of the alginate, which was dominant above the optimum ratio, thus creating a high density of nuclei, allowing aggregation to occur. A lower ratio not only led to a higher tendency to produce larger particles, but also a higher probability of anisotropic particle shape formation due to the lack of reducing capability of the alginates.

Keywords: *alginate, microwave irradiation, particle size, reducing and stabilizing agent, silver nanoparticles (Ag-NPs).*

1 Introduction

Silver nanoparticles (Ag-NPs) have attracted significant interest of researchers due to their excellent optical and electrical properties. The optical properties can be explained by the phenomenon of the coupling of incident electromagnetic radiation into a surface plasmon (described as a collective oscillation of the conduction electrons). The coupling occurs at the interface between the particle and the medium surrounding the particle, yielding a strong absorption band in the visible light spectrum. This collective oscillation of the free electrons is

Received February 21st, 2014, Revised November 11th, 2014, Accepted for publication February 5th, 2015.
 ISSN: 2337-5760, DOI: 10.5614/j.math.fund.sci.2015.47.1.3

sensitive to changes in the size of the particles, thus by varying the size of the particles, the optical properties can be tuned [1-2].

These properties make it possible to apply Ag-NPs in a wide range of areas, such as in optical sensors [3-4] or as substrate for surface-enhanced Raman spectroscopy (SERS) [5-6]. Since at the nano scale the reactivity is enhanced significantly, this property allows Ag-NPs to be an effective catalyst for many chemical reactions [7-8]. Ag-NPs are also known to have antimicrobial and antifungal properties and have been widely applied in wound-care products and medical devices, including dental work and catheters [9]. Some researchers have shown other potential applications of Ag-NPs, as adsorbent [10-12] or as dual functional adsorbent-catalyst[13].

Stability is one of the great challenges of particles at very small sizes. Stabilization of nanoparticle dispersion is difficult due to the high surface area to volume ratio and the high surface energy of the nanoparticles. Modification of nanoparticles with an appropriate stabilizing material can solve this problem. Generally, materials such as surfactants, polymers and ligands can act as capping agent for nanoparticles and have been proven to successfully prevent the particles from aggregating. Previous studies have shown that several polymers, such as poly(vinyl alcohol) (PVA) [12], polymethyl-methacrylic acid (PMMA) [13], polyethylene glycol (PEG) [3], polyvinylpyrrolidone (PVP) [14-15], can play a significant role as stabilizers for silver nanoparticles.

The fact that surfactants or ionic polymers can be strongly attached to the nanoparticle surface and cannot be easily removed from it is another problem that is sometimes encountered. Stabilizers may affect the physicochemical properties of the obtained nanoparticles. Therefore it is crucial to find an appropriate stabilizing agent that supports the nanoparticle function.

Since Ag-NPs are widely applied in the biomedical field, there is a growing need to develop environmentally friendly processes for nanoparticle synthesis that do not use toxic chemicals, applying biodegradable and biocompatible materials instead. Silver nanoparticle synthesis involving bioreduction using part of a plant or a plant extract has been suggested as a possible ecofriendly alternative to chemical and physical methods [16-17].

Biopolymers extracted from a plant, algae, or part of an animal body have great potential, both as reducing agent and stabilizer, since they usually have a bulky structure and many functional groups that have reducing capability, such as carbonyl, alcohol, aldehyde, amine and carboxylate. Synthesis of silver nanoparticles by biopolymers such as cellulose [18], starch [19], guar gum [6],

gum kondagogu [20], gum olibanum [21], chitosan [22], [9], and alginate-chitosan [23] have been reported.

Alginates are generally referred to as a family of polyanionic biopolymers derived from marine kelp, mainly from brown sea algae. Alginates consist of two basic building blocks, α-L-guluronic acid (G) and β-D-mannuronic acid (M) residues, linearly linked together by 1-4 linkages [24]. Some researchers have studied the synthesis of Ag-NPs using alginate under gamma irradiation [25], UV photoactivation [26], and conventional heating at a certain temperature [27]. In the case of gamma irradiation and photoactivation techniques, the cost of the process is a critical aspect that should be considered, especially if synthesis will be applied on an industrial scale. Microwave dielectric heating has the advantage that the reaction proceeds at higher reaction rates and selectivities as compared to conventional heating [28]. Therefore, this synthesis technique seems to have potential for metal nanoparticle synthesis.

Hereafter, we report the synthesis and characterization of silver nanoparticles using alginate as both reducing and stabilizing agent with the aid of microwave irradiation. Although many researches have reported that the concentration ratio of metal precursor/alginate controls the silver nanoparticle morphologies, the effect of pH and ionic strength in the case of Ag-NP synthesis using alginate has not been discussed in detail. This study revealed that pH and ionic strength have a great influence on the characteristics of the obtained nanoparticles, including particle size and shape, and polydispersity. We propose that the silver nanoparticles are stabilized sterically and electrostatically by the bulky structure of the alginate molecules and the negative charge of their carboxyl groups.

2 Material and Methods

$AgNO_3$ was obtained from Merck. Sodium alginate was obtained from Himedia. HCl and NaOH (from Merck) were used for adjusting pH. The solvent used in this study was double distilled water (PT. Ikapharmindo). All of the chemicals used in this study were of analytical reagent grade.

Synthesis of Ag-NP was conducted in a domestic microwave oven with a total power of 800 Watt, which could be adjusted to 30%, 50%, 80% and 100% of the total power. Briefly, 1 mL of $AgNO_3$ solution was poured into a 100 mL beaker glass and added by 5 mL of alginate solution and diluted with double distilled water until a total volume of 20 mL. The mixture was irradiated for some minutes until the color of the colloid solution changed from colorless to yellowish brown. The final colloid solution was cooled in room temperature before further characterization. Synthesis of Ag-NP was also conducted by conventional heating, by heating the mixture using a hotplate at a temperature

of 70-80°C. The characteristics of the product were compared with those produced by the microwave irradiation technique.

The optical extinction spectra were measured by an ultraviolet-visible (UV-Vis) spectrophotometer (UV-1700, Shimadzu) in a scanning range of 190 nm to 1100 nm. The morphologies of the Ag-NP were observed by transmission electron microscopy (TEM) on a JEM-1400 electron microscope JEOL instrument operating at an accelerating voltage of 120 kV. The particle size and particle size distribution were evaluated with a particle size analyzer (Malvern Zetasizer, ZEN-1600). Interaction between Ag-NP and alginate was confirmed by Fourier transform infrared spectroscopy (FTIR), IR-Prestige-21, Shimadzu.

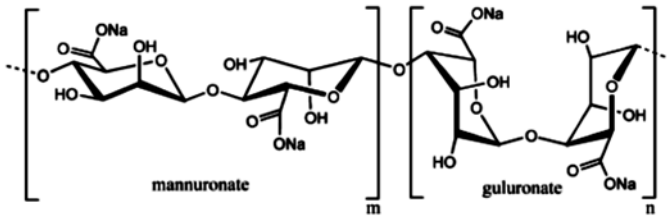

Figure 1 Chemical structure of alginate.

3 Result and Discussion

In this experiment, alginate (the structure is shown in Figure 1) was utilized as the reducing agent, replacing a chemical reducing agent that may possess toxicity, so that the as-prepared Ag-NP is applicable in a wide range of areas, including the biomedical field.

Ag-NP formation via reduction by alginate can be monitored visually by observing the change of the colloid solution color from colorless to bright yellow and subsequently to light brown, depending on the reaction conditions. The UV-Vis spectrum of the Ag-NP showed a characteristic peak at about 400 nm, which can be attributed to the surface plasmon resonance (SPR) for spherical Ag-NP (Figure 2). The peak at about 300 nm in the UV-Vis spectrum of silver nitrate had disappeared, indicating that Ag^{+} was completely reduced to Ag^{0}. The intensity and position of the shoulder of the alginate spectrum at about 290 nm was slightly shifted, confirming that there had been interaction between the polymer and the metal precursor. The presence of Ag-NP in the alginate matrix was supported by the EDX analysis, which showed 6.94 % wt of Ag and large amounts of C and O.

Compared to conventional heating, microwave irradiation is more advantageous due to homogeneous heating and fast nucleation, leading to a smaller particle

size and a narrower size distribution [29]. In this experiment, conventional heating was compared to microwave irradiation in the Ag-NP synthesis. The concentration of each reagent and the concentration ratio of alginate/metal precursor and pH were kept constant in order to elaborate the effect of these two techniques on the characteristics of the as-synthesized Ag-NPs. By employing the microwave irradiation technique, the Ag-NP synthesis was completed in only 1-2 minutes, whereas by conventional heating it took longer (30 minutes) to achieve the same absorbance value and thus the same concentration (assuming that the absorbance is linearly correlated with the Ag-NP concentration).

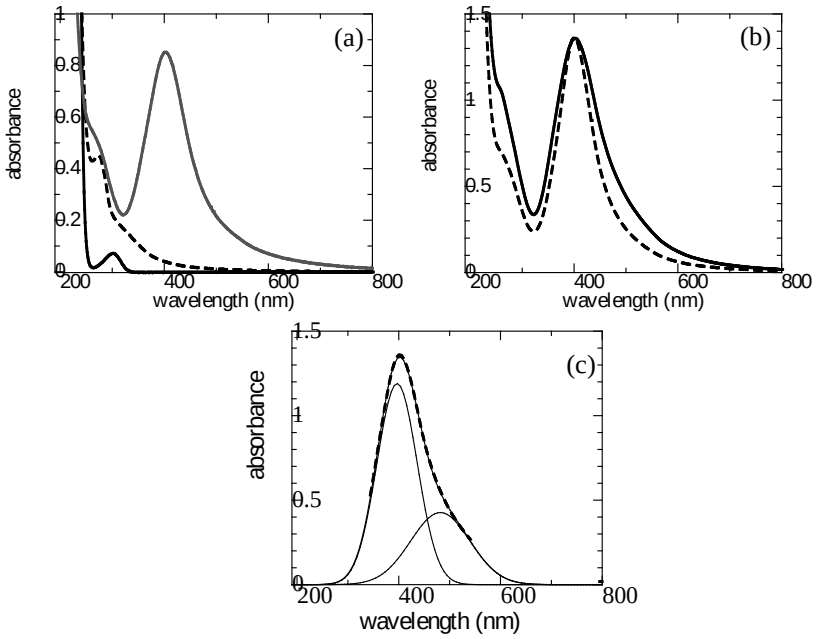

Figure 2 UV-Vis spectrum of $AgNO_3$ (—), alginate (- - -), and Ag-NP synthesized by alginate (— · —) (a). SPR spectra of 0.5 mM Ag-NP synthesized using 0.0375 %w/v alginate by microwave irradiation (- - - -) and conventional heating (—) at pH 10 (b). Gaussian fitting analysis of SPR spectrum of Ag-NP synthesized using alginate by conventional heating (c).

From the UV-Vis spectrum (Figure 2(a) and 2(b)), it can be seen that the peak of the Ag-NP synthesized by conventional heating was broadened at longer wavelengths, indicating that there was another peak overlapping with the first peak (at about 400 nm). Further analysis using a Gaussian fitting program showed two peaks overlapping each other (Figure 2(c)). There are two possibilities regarding the presence of two peaks in the SPR spectrum. Firstly, it may be a contribution of larger particles, as they exhibit radiation absorption at

longer wavelengths. Secondly, it may indicate the presence of nonspherical particles. Many researchers have reported the SPR characteristics of nonspherical particles, including rod, triangular, and cubic shapes, and found that these particles exhibit two SPR peaks, i.e. transversal and longitudinal SPR peaks. The first peak, at a shorter wavelength, is attributed to the transversal SPR peak, while the second peak, at a higher wavelength, is attributed to the longitudinal SPR peak. A longer distance between both peaks indicates a higher aspect ratio [30-31]. The broadened peak was not observed in the spectrum of the Ag-NPs synthesized by microwave irradiation, suggesting that the microwave irradiation was able to produce more homogeneous Ag-NPs, both in size and shape.

Table 1 Particle size and its distribution of Ag-NPs synthesized by microwave and conventional heating.

Synthesis technique	Particle size (nm)	% volume	Width (nm)
Microwave irradiation	1.782	99.4	1.202
Conventional heating	8.766	71.4	2.261
	46.65	28.1	32.0

The characterization results of the Ag-NPs by particle size analysis (Table 1) supported the above statement. The particle size of theAg-NP synthesized by microwave irradiation was smaller than that synthesized by conventional heating, and the size monodispersity was higher for the former, as confirmed by the high value of percentage volume (> 99%). The polydispersity of theAg-NP synthesized by conventional heating can be clearly observed by its two kinds of particle sizes (8.766 and 46.65 nm) or bimodal curve of particle size (not shown here).

3.1 Effect of Ag Precursor Salt Concentration

Generally, the higher the concentration ratio of metal precursor salts/polymer, the larger the particle size and the broader the size distribution. This can be explained by the higher number of nuclei that are formed at higher concentrations of the metal precursor salt. Apart from that, the fraction of uncapped nanoparticles increases with the increase of the ratio, leading to a higher tendency of the particles to interact with each other.

The SPR spectra of the Ag-NPs changed significantly in peak intensity and shape with the change of the Ag^+ concentration (the alginate concentration was kept constant), as shown in Figure 3(a). At an Ag^+ concentration of 0.125 mM, a very low absorbance and broad peak at 409 nm implied that Ag-NP formation was not effective. With the increase of the Ag^+ concentration to 0.250 mM, the absorbance increased significantly and formed a well-defined peak with the

maximum at 403 nm. At an Ag^+ concentration of 0.50 mM, the wavelength shifted to 400 nm and the absorbance significantly increased. It could be expected that the particle size of Ag-NP was smaller and the quantity of those particles was higher as the concentration of Ag^+ increased from 0.125 to 0.50 mM. The results of the particle size measurement supported this prediction (Figure 3(b)). The particle size and its peak width decreased, accompanied by an increase in percentage volume, as the Ag^+ concentration was increased from 0.125 mM to 0.50 mM.

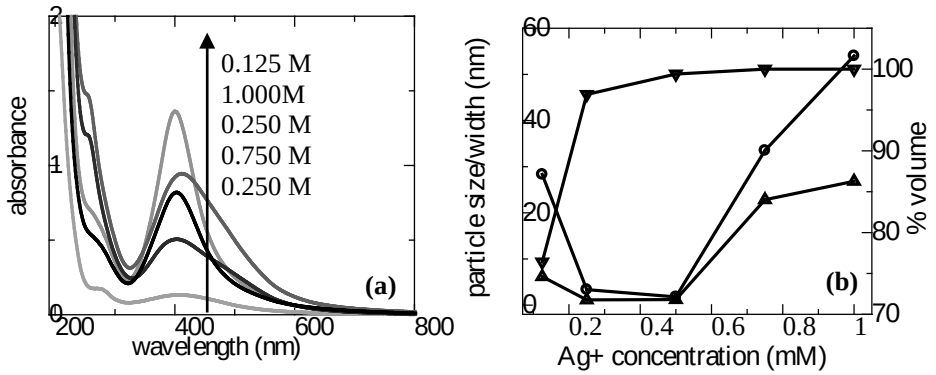

Figure 3 SPR spectra of Ag-NP synthesized using alginate at various [Ag^+] (alginate concentration = 0.0375 %w/v) (A).Plot of particle size (—▲—), peak width (—◆—) and % volume (—■—) as a function of [Ag^+] (alginate concentration = 0.0375 %w/v) (B).

This trend changed at an Ag^+ concentration higher than 0.50 mM. The absorbance value of the SPR peak decreased with the increase of the Ag^+ concentration and the peak was broadened at higher wavelengths. Further analysis using a Gaussian fitting program showed that those peaks consisted of two overlapping peaks with a maximum wavelength of 403 nm and 495 nm (for 0.75 mM Ag^+) and of 398 nm and 501 nm (for 1.00 mM Ag^+).

As shown in Figure 3(b), the particle size significantly increased with the increase in Ag^+ concentration, from 0.50 mM to 1.00 mM, but the value of percentage volume did not change significantly. This was probably due to a coalescence process that produces large aggregates and, under certain conditions, nonspherical particles.

Particle size measurement in this experiment was performed using a particle size analyzer that works based on light scattering. This instrument has limitations, especially in its incapability to confirm particle shape. It is widely known that the Mie scattering equation is derived from the approximation of a

spherical particle. Thus, supporting data from another technique for morphology analysis is helpful for characterization of the obtained nanoparticles.

Figure 4 represents a TEM image of Ag-NP synthesized at an Ag^+ concentration of 0.50 and 2.50 mM. Larger and anisotropic particles (cube, rod-like, truncated triangular and truncated rhombus) could be found at higher Ag^+ concentrations. At a constant alginate concentration, a higher Ag^+ concentration means a lower ratio of alginate/Ag^+ (metal precursor) and the probability of anisotropic shape particles formation increases. Wang, *et al*. [32] and Hoppe, *et al*. [14] also found this trend in the synthesis of gold and silver nanoparticles in the presence of poly(vinylpyrrolidone), respectively.

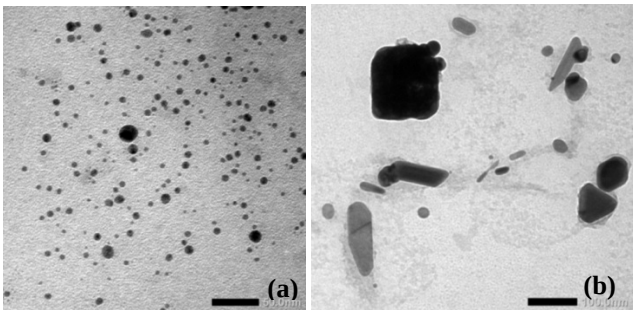

Figure 4 TEM image of Ag-NP at [Ag^+] = 0.50 mM (a) and 2.50 mM (b) (alginate concentration = 0.0375 %w/v).

As the alginate concentration remained constant, the amount of available reducing groups of alginate did not alter, so that the stabilization of Ag-NP was solely controlled by the Ag^+ concentration. This result also shows that the Ag^+ concentration played a role as morphology-controlling agent.

3.2 Effect of Alginate Concentration

Figure 5 shows that at a constant concentration of silver nitrate, a change of the alginate concentration could change the characteristics of the as-prepared Ag-NPs. In this synthesis, the alginate played a role both as reducing agent and stabilizer, so that a change in alginate concentration could change these two capabilities.

Several studies have explained that in the case where polymers only act as capping agent for metal nanoparticles, the higher the polymer concentration or the concentration ratio of polymer/metal precursor, the larger the inhibition effect on the agglomeration of particles [33-34]. This effect may come from a steric effect from the bulky structure of the polymers.

From Figures 5(a) and 5(b), it can be seen that there was an increase in absorbance with the increase in alginate concentration until a value of 0.05 %w/v. This can be interpreted as follows: a higher alginate concentration means a higher amount of reducing groups that can interact with the metal precursor salt, leading to a high amount of nanoparticles yielded from the process. The absorbance values at an alginate concentration of 0.025 and 0.0375 %w/v were similar but had a different peak width. The SPR peak at an alginate concentration of 0.025 %w/v was wider than that of 0.0375 %w/v, indicating that the polydispersity of the former was higher than that of the latter.

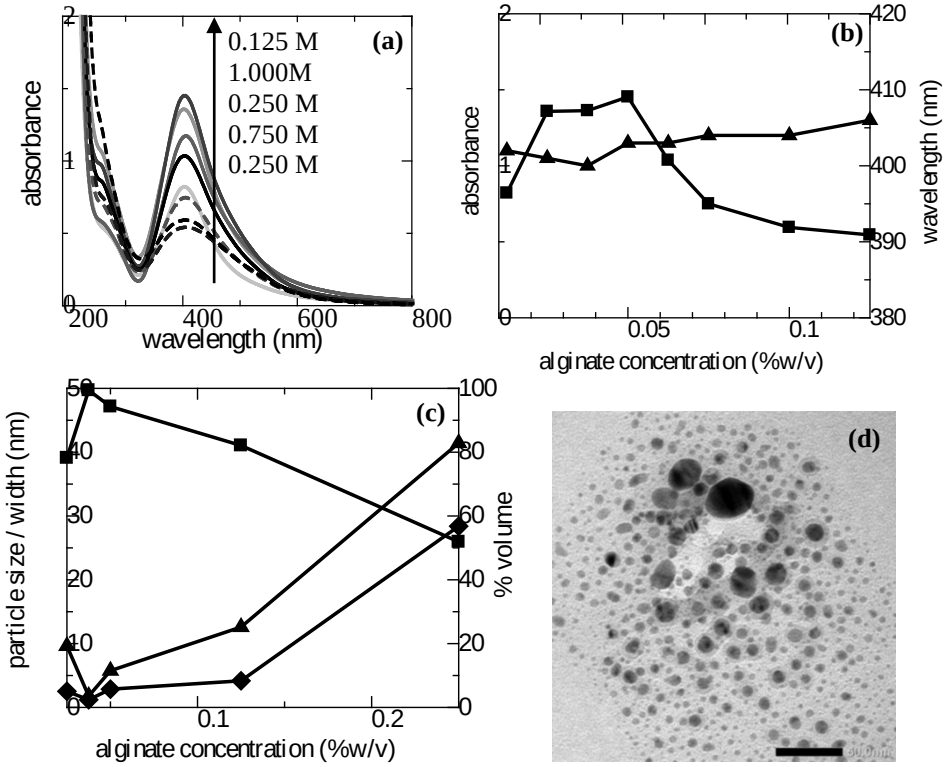

Figure 5 SPR spectra of Ag-NP synthesized using alginate at various alginate concentrations (a). Plot of absorbance (—■—) and wavelength (—▲—) as a function of alginate concentration (b). Plot of particle size (—▲—), peak width (—◆—) and % volume (—■—) as a function of alginate concentration (c).TEM image of Ag-NP at an alginate concentration of 0.25 %w/v (in all variations, $[Ag^+]$ = 0.50 mM) (d).

At a constant Ag^+ concentration, a higher alginate concentration means a higher concentration ratio of polymer/metal precursor salts. As stated above, it could be expected that a higher alginate concentration resulted in a better capability of

stabilizing the Ag-NP due to a higher steric effect. Surprisingly, in this experiment we found that at an alginate concentration of 0.05 %w/v, the absorbance decreased with an increase of the alginate concentration. It can be assumed that this decrease of absorbance was related to the decrease in SPR characteristic of Ag-NP and the increase of contribution of radiation absorption by the alginate. It is deeply known that the thickness of the shell influences the oscillation of the electrons due to the interaction with capping agents [35]. On the other hand, aggregate formation occurred in this case, as supported by the results of the particle size measurement.

Figure 5(c) shows a drastic increase in Ag-NP size at alginate concentrations higher than 0.05 %w/v. A broad size distribution could also be observed from a low value of percentage volume and a high value of peak width. This phenomenon indicates that the growth mechanism of the nanoparticles not only involved a coalescence process, but also proceeded via Ostwald ripening, especially at the particle surface that was not perfectly capped by alginates.

Figure 5(d) shows a TEM image of the Ag-NP at an alginate concentration of 0.25 %w/v. It clearly shows that the density of the particles was so high that each particle was only separated from the other by a short distance. The small particle-particle separation distance led to a higher tendency of the particles to interact with their neighbours, forming larger particles or aggregates. The large particles could act as seeds for growth for other particles and subsequent larger aggregates would be formed. This phenomenon cannot be explained by the role of the alginate as stabilizer, since the higher the concentration of stabilizer, the smaller the particle size. As the alginate also acts as reducing agent, an increase in alginate concentration resulted in a higher amount of reducing groups. Consequently, those reducing groups produced a high density of nuclei in this system.

3.3 Effect of pH

The effect of pH on the characteristics of Ag-NP was studied over a wide range of pH values, but the formation of Ag-NP was only effective in basic condition. Figure 6(a) shows that at pH 7.0 and 8.0 the colloid solution was colorless and the yellowish brown color emerged at aminimum pH of 9.0. The higher the pH, the more intense the color, indicating that the formation of Ag-NP was more effective.

UV-Vis spectra analysis showed that at pH 10.0 the intensity of the spectrum was significantly higher, indicating that a large amount of Ag-NP was yielded in this condition. The intensity drastically decreased with the decrease of pH, and at a pH of around 9.0 the peak was only a shoulder (Figure 6(b)). Besides

the intensity decrease, there was a shift in the wavelength and peak width. With the decrease of pH, red shift and peak broadening occured. Since the peaks were not symmetric and tended to form a tail at longer wavelengths, the above phenomenons can be attributed to larger particle size and broader size distribution.

The experimental results suggest that the dominant anionic form of hydroxyl and carboxyl groups at a high pH significantly contribute to the Ag-NP formation. The effect of pH on Ag-NP formation was previously studied by Amaladhas, *et al*. [36], utilizing biomolecules from *Cassia angustifolia* extract as reductant and stabilizer in the synthesis of Ag-NP. In that research, the Ag-NP formation in basic condition proceeded readily. In this condition, the nucleation rate was so high that the particles had no time to interact with each other and form aggregates. Consequently, a smaller particle size and narrower size distribution could be obtained. Our results are in good agreement with this previous study.

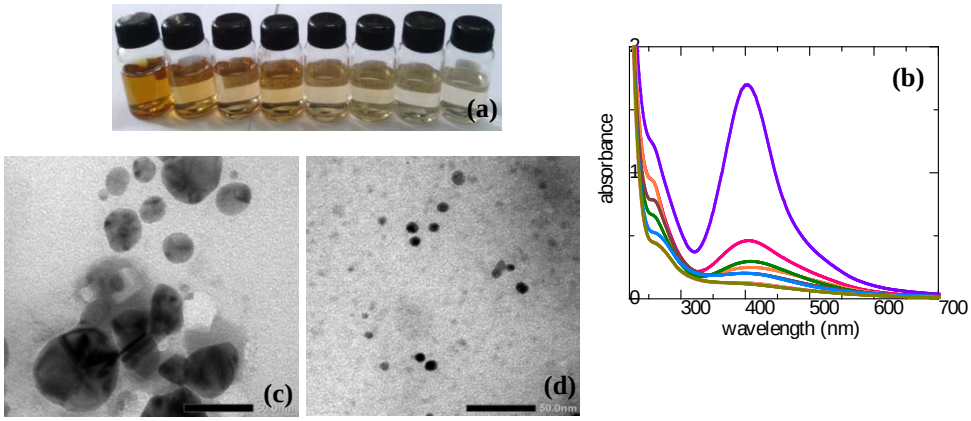

Figure 6 Colloid solution of Ag-NP synthesized by alginate at various pH (10.0, 9.8, 9.6, 9.4, 9.2, 9.0, 8.0, 7.0 from left to right) (a).SPR spectra of Ag-NP synthesized by alginate at various pH (10.0, 9.8, 9.6, 9.4, 9.2, 9.0 from top to bottom) (b). TEM image of Ag-NP at a pH of 9.0 (c) and 12.0 (d), respectively (in all pH, $[Ag^+]$ = 0.50 mM, [alginate] = 0.0375 %w/v).

It is known that E^0, the standard redox potential of reactions that involve H^+ and OH^- ions, is highly dependent on pH. The changes in the redox potential of the reducing species affect the ΔE^0 of the overall redox reaction, causing changes in the supersaturation concentration of the metal atoms and, consequently, in the nucleation rate which controls the final particle size. In the case of an ascorbic/dihydroascorbic system, an increase in the concentration of protons

reduces the ability of the oxidized species to supply electrons, causing a significant slowdown of the reduction reaction [37].

It can be suggested that at pH 9.0 or lower, the reducing capability of the alginate is lower than that at a higher pH. Consequently, the nucleation rate is slower and a large fraction of the precursor salt has not reduced yet and still remains as ions, trapped in the alginate bulky structure. This is supported by the results of the particle size measurement, which showed a large size (140 nm) of Ag-NP at pH 9.0. This value may be interpreted as the size of alginate particles that have formed clusters containing Ag^+ ions or Ag-NP nuclei in their matrix. On the other hand, the slower nucleation rate tends to form larger particles due to uncontrolled growth of the nuclei. The TEM image of Ag-NP at this pH clearly reveals these large aggregates (Figure 6(c)).

Furthermore, a lower pH means that more carboxyl groups are in the protonated forms, so it can be predicted that a large amount of hydrogen bonds are present. The particle-particle separation distance of the alginates was shorter due to these bonds, leading to the formation of large aggregates. Conversely, at a higher pH, anionic forms of the carboxyl groups are abundant and the negative charges will repel each other, yielding a longer particle-particle separation distance of the alginate. The repulsion prevents interparticle attraction of nanoparticles, resulting in a higher electrostatic stabilization and consequently, a smaller particles size (Figure 6(d)). This is similar to the statement by Amaladhas, *et al*. [36] that –COO- groups in the biomolecules played a great role in stabilizing the as-prepared silver nanoparticles.Tripathy, *et al*. [38] also found that the stability of Ag-NP synthesized by aqueous extract of *Azadirachta indica* (Neem) leaves was enhanced at alkaline pH range owing to complete charging of the clusters, thus maximizing the repulsive electrostatic interactions. The repulsive electrostatic interaction in this experiment was confirmed by the zeta potential value, which was relatively high at pH 10 (-20.3 mV).

3.4 Effect of NaCl Concentration

Figure 7(a) and 7(b) show that the absorbance of the SPR peak decreased with the increase of the NaCl volume, indicating that the amount of Ag-NP was reduced as the interaction with the salts became more intense. The chloride ions may compete with the alginate to react with silver ions. Moreover, the NaCl concentration clearly influenced the characteristics of the as-synthesized AgNP, since a higher concentration means a higher ionic strength and the latter was responsible for causing the electrical double layer to move closer to the particle surface and shrinks in size, which results in the decrease of debye length. Thus, adsorption of ions onto the surface of silver particles and thereby changing the surrounding dielectric environment results in the observed blue-shift in the SPR

absorption peaks (Figure 7(a) and 7(b)).This is also supported by earlier observations of the ionic strength effect on the SPR absorption peaks of gum acacia-capped silver nanoparticles [39]. The decrease of particle size (Figure 7(c)) was probably due to the slower formation rate of nanoparticles, since in this case, the formation rate was linearly correlated with the particle size. This phenomenon is also obtained in the Fe_3O_4 nanoparticle synthesis [40].

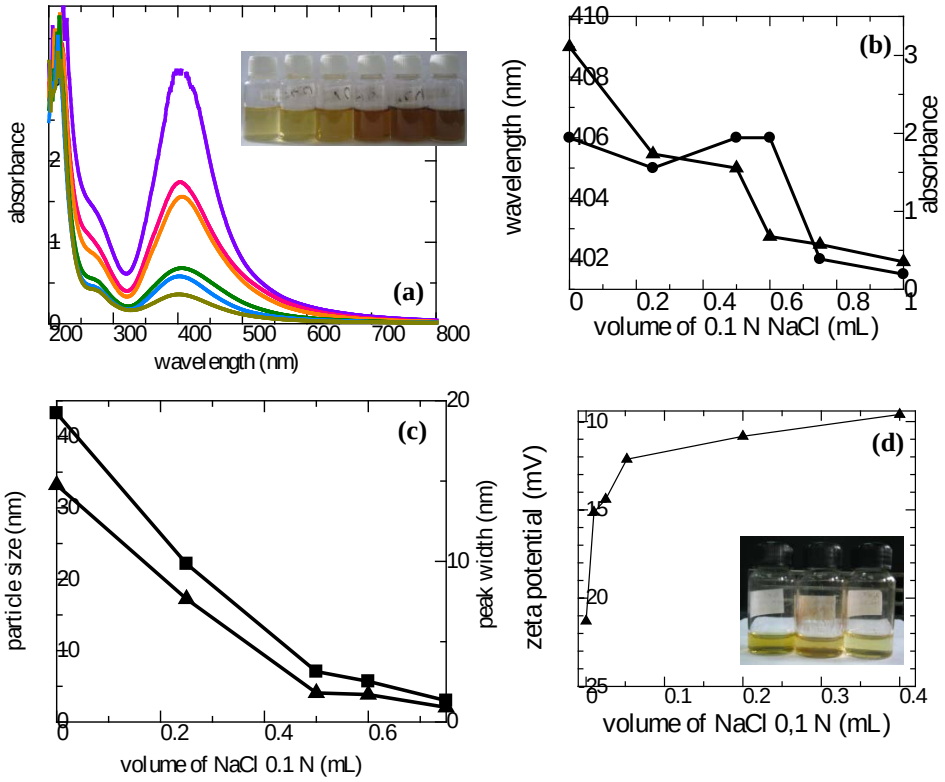

Figure 7 SPR spectra of Ag-NP synthesized by alginate at various volumes of 0.10 N NaCl (0.0, 0.25, 0.50, 0.60, 0.75, 1.00 mL from top to bottom) ($[Ag^+]$ = 0.50 mM, [alginate] = 0.075 %w/v). Insert: colloid solution of Ag-NP (0.0, 0.25, 0.50, 0.60, 0.75, 1.00 mL 0.10 N NaCl from right to left). Plot of wavelength (—■—) and absorbance (—▲—) (a), plot of particle size (—■—) and peak width (—▲—) (b),plot of zeta potential(c)as a function of volume of 0.10 N NaCl (d). Insert: colloid solution of Ag-NP (0.50, 0.60, 1.00 mL 0.10 N NaCl from right to left) after 1 month.

In this system, the zeta potential decreased as the ionic strength increased (Figure 7(d)). This can be used to estimate the repulsion energy between Ag nanoparticles by using the classical Derjaguin-Landau-Verwey-Overbeek

(DLVO) theory. According to this theory the repulsion energy between nano-colloids decreases as the ionic strength increases, resulting in a decrease of colloidal stability [41]. Visual observation of the Ag-NP synthesized in the presence of NaCl shows sedimentation of Ag-NP aggregates at high NaCl concentrations (Figure 7(d) insert).

3.5 FTIR Characterization

Interaction of Ag-NP with alginate was confirmed by FTIR spectrum analysis (Figure 8). In the FTIR spectrum of the alginate, the peak between 3200-3600 cm^{-1} can be assigned to the stretching vibration of O-H groups, while the sharp peaks at 1412 cm^{-1} and 1591 cm^{-1} correspond to –COO- symmetric and asymmetric stretching, respectively. A small and broadened peak in the range of 1327-1370 cm^{-1} can be attributed to C-O stretching. The two peaks at wavelengths of 1016.5 and 1078 cm^{-1} correspond to C=O and C-O-C stretching. C-O stretching for alcohol occurred at the absorption peak at 1150 cm^{-1}. The absorption peaks in the range of 1030-1200 cm^{-1} are characteristics of natural polysaccharide.

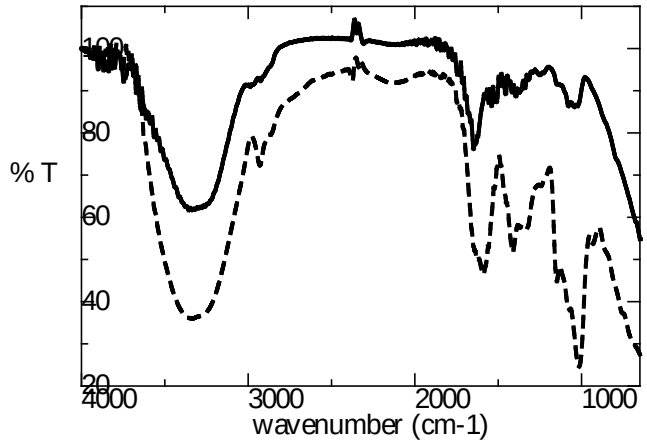

Figure 8 FTIR spectra of alginate (- - -) and Ag-NP synthesized by alginate (—).

By comparing the FTIR spectrum of the alginate with that of the Ag-NP, it can be observed that there was a significant shift of wavelength position from 1591 cm^{-1} for the alginate to 1640 cm^{-1} for the Ag-NP, followed by a decrease in intensity. This shift confirms the interaction between oxygen of carboxyl groups in the alginate structure with the Ag-NP. The peak shift in the range of 3200-3500 cm^{-1} was not significant, but the decrease in intensity was sharp. The shift in position and intensity was related to the probability of interaction

between Ag-NP and the hydroxyl groups of alginate. The single, broadened peak from 1017 to 1084 cm^{-1} can be assigned to the chemical transformation during the reduction process of Ag^{+} to Ag^{0}.

3.6 Reduction and Stabilization Mechanism

From the FTIR results it can be inferred that the interaction between Ag-NP and oxygen from the carboxyl and hydroxyl functional groups of alginate to form complexes occurred during synthesis. The complex formation was also supported by the blue-shift in the UV-Vis spectrum of Ag-NP at pH 9.0. Since the Ag-NP has not significantly formed yet at this pH, it can be assumed that the complex formation occurred before the reduction reaction of Ag^{+} to Ag^{0} took place.

Table 2 Comparison between several biopolymer-based nano silver synthesis.

Biomaterial	Synthesis technique	Particle size (nm)	Particle shape	Optimum interaction time
Aqueous extract of *Azadirachtaindica* (Neem) leaves (R&S) [38]	incubated in rotary shaker at 120 rpm	10-20	spherical	4 h
Starch(S) D-glucose (R) [5]	ultrasound	14.4 ± 3.3	mostly spherical, few nanorods	1 h
Gum olibanum (Boswelliaserrata) (R & S) [21]	autoclave at 121°C and 103 kPa	7.5 ± 3.8	spherical	30 min
Gum kondagogu (Cochlospermumgossypium) (R&S) [20]	autoclave at 121°C and 15 psi	about 11.2 and 4.5[a] 3 (nearly 70%)[b]	spherical	30 min 60 min
Cyamopsistetragonaloba (guar gum) (R&S) [6]	magnetic stirring at 70°C	~8	spherical	90 min
Calcium alginate (S) [26]	photochemical	<10	spherical	40 min
Sodium alginate (S) [23]	γ-irradiation	6-30	spherical, with a small portion of triangular	not mentioned
Cassia angustifolia (R&S) [36]	sunlight-induced	9-31 (avg. 21.6)	spherical	10 min
Sodium alginate (R&S)*	microwave irradiation	3.564	spherical	2 min

S = stabilizer, R = reducing agent, [a] 30 min, [b] 60 min, * in this study

By monitoring the particle size and the SPR spectrum of the as-synthesized Ag-NP, it was suggested that the stabilization step involved intermolecular force breaking of the alginate followed by a rearrangement of the alginate layer on the particle surface that protected them from coalescence. Electrostatic repulsion from the anionic carboxyl groups also contributed to the stabilization step, as

supported by information that confirms the effective formation of small spherical particles at high pH.

The synthesized Ag-NPs have interesting optical properties, thus enabling this material to be employed as optical sensor, for example to analyze heavy metals in the environment. In this case, a wavelength shift of the SPR spectrum could be observed and the peak absorbance had a linear relation with the analyte concentration, thus providing quantitative analytical information. Besides, the Ag-NP synthesis was done in the absence of toxic materials, thus allowing the nanomaterial to be applied in the biomedical field.

Several studies that employed biopolymers as stabilizer or as both reducing agent and stabilizer can be compared with the result of this study, as shown in Table 2. In most of the experiments a long reaction time was necessary to achieve optimum condition. It can clearly be seen that the Ag-NP synthesized by microwave irradiation only needed a very short time to produce small homogeneous nanoparticles. Different from aqueous extracts of parts of plants, which contain several compounds, the alginate is a pure compound, purified from the extract of marine brown algae. Thus, controlling the reaction, such as via adjusting the pH, is easily conducted, yielding characteristics of the product as expected, since there is a low matrix effect. Moreover, the alginate is applicable in various fields, including the biomedical field, thus allowing the as-synthesized Ag-NP to be employed in those fields.

4 Conclusion

Green and facile synthesis of Ag-NPs was conducted by employing an alginate and a microwave irradiation technique. The alginate had a dual function as both reducing agent and stabilizer. The concentration ratio of alginate/metal precursor salts greatly influenced the particle size of the Ag-NP and its distribution. A higher ratio yielded better stabilization until a certain ratio. Above this limit, the higher the ratio, the more dominant the role of the alginate as a reducing agent over its role as a stabilizing agent, leading to a higher density of nuclei and subsequent aggregation. The probability of anisotropic particle shape formation was higher at lower ratios. The morphologies of the Ag-NP were also significantly dependent on pH and ionic strength. Higher values of both of them were responsible for producing a smaller particle size and a narrower size distribution. Therefore, we found the possibility of controlling nanoparticle size, shape and monodispersity by adjusting the alginate/metal precursor concentration ratio, pH and ionic strength. Such an environmentally-friendly and facile synthesis method for silver nanoparticles may have great potential in large-scale manufacturing to match the increasing commercial and industrial demands, especially in the biomedical field.

Acknowledgements

This work was financially supported by: 1) Hibah Riset Madya from the Directorate of Research and Community Services, Universitas Indonesia, Indonesia (No.2179/H2,R12/HKP.05.00/2012), 2) the Training and Education Center, Ministry of Industry, Indonesia.

References

[1] Murugadossa, A., Goswamia, P., Paul, A. & Chattopadhyay, A., *'Green' Chitosan Bound Silver Nanoparticles for Selective C–C Bond Formation Via In Situ Iodination of Phenols*, J. Mol. Catal. A: Chemical, **304**(1-2), pp. 153-158, 2009.

[2] Li, W., Sun, C., Hou, B. & Zhou, X., *Room Temperature Synthesis and Catalytic Properties of Surfactant-Modified Ag Nanoparticles*, Int. J.Spect., pp. 1-7, 2012.

[3] Li, W., Guo, Y. & Zhang, P., *SERS-Active Silver Nanoparticles Prepared by a Simple and Green Method*, J. Phys. Chem. C, **114**(14), pp. 6413-6417, 2010.

[4] Stamplecoskie, K.G., Scaiano, J.C., Tiwari, V.S. & Anis, H., *Optimal Size of Silver Nanoparticles for Surface-Enhanced Raman Spectroscopy*, J. Phys. Chem. C, **115**(5), pp. 1403-1409, 2011.

[5] Vasileva, P., Donkova, B., Karadjova, I. & Dushkin, C., *Synthesis of Starch-Stabilized Silver Nanoparticles and their Application as a Surface Plasmon Resonance-Based Sensor of Hydrogen Peroxide*, Colloids Surf. A: Physicochem. Eng. Aspects, **382**(1-3), pp. 203-210, 2011.

[6] Pandey, S., Goswami, G.K. & Nanda, K.K., *Green Synthesis of Biopolymer-Silver Nanoparticle Nanocomposite: An Optical Sensor for Ammonia Detection*, Int. J. Biol. Macromol., **51**(4), pp. 583-589, 2012.

[7] Lara, H.H., Garza-Treviño**,** E.N, Ixtepan-Turrent, L. & Singh**,** D.K., *Silver Nanoparticles are Broad-Spectrum Bactericidal and Virucidal Compounds*, J. Nanobiotechnol., **9**(30),pp.1-8,2011.

[8] Seredych, M., Bashkova, S., Pietrzak, R. & Bandosz, T.J., *Interactions of NO_2 and NO with Carbonaceous Adsorbents Containing Silver Nanoparticles*, Langmuir, **26**(12), pp. 9457-9464, 2010.

[9] Saifuddin, N., Nian, C.Y., Zhan, L.W. & Ning, K.X., *Chitosan-silver Nanoparticles Composite as Point-of-use Drinking Water Filtration System for Household to Remove Pesticides in Water*, Asian J.Biochem., **6**(2), pp. 142-159, 2011.

[10] Sumesh, E., Bootharaju, M.S.,Anshup & Pradeep, T., *A Practical Silver Nanoparticle-Based Adsorbent for the Removal of Hg^{2+} from Water*, J. Hazard. Mater, **189**(1-2), pp. 450-457, 2011.

[11] Baek, S.-W., Kim, J.-R. & Ihm, S.-K., *Design of Dual Functional Adsorbent/Catalyst System for the Control of VOC's by Using Metal-Loaded Hydrophobic Y-Zeolites*, Catal. Today, **93-95**(82), pp. 575-581, 2004.

[12] Porel, S., Ramakrishna, D., Hariprasad, E., Gupta, A.D. & Radhakrishnan, T.P., *Polymer Thin Film With In Situ Synthesized Silver Nanoparticles as a Potent Reusable Bactericide*, Curr. Sci., **101**(7), pp. 927-934, 2011.

[13] Singh, N. & Khanna, P.K., *In situ Synthesis of Silver Nanoparticles in Polymethylmethacrylate*, Mater. Chem. Phys., **104**(2-3), pp. 367-372, 2007.

[14] Hoppe, C.E., Lazzari, M., Pardiñas-Blanco, I. & López-Quintela, M.A., *One-Step Synthesis of Gold and Silver Hydrosols Using Poly(N-vinyl-2-pyrrolidone) as a Reducing Agent*, Langmuir, **22**(16), pp. 7027-7034, 2006.

[15] Noroozi, M., Zakaria, A., Moksin, M.M., Wahab, Z.A. & Abedini, A., *Green Formation of Spherical and Dendritic Silver Nanostructures under Microwave Irradiation without Reducing Agent*, Int. J. Mol. Sci.,**13**(7), pp. 8086-8096, 2012.

[16] Iravani, S., *Green Synthesis of Metal Nanoparticles using Plants*, Green Chem., **13**(10), pp. 2638-2650, 2011.

[17] Salam, H.A., Rajiv, P., Kamaraj, M., Jagadeeswaran, P., Gunalan, S. & Sivaraj, R., *Plants: Green Route for Nanoparticle Synthesis*, Int. Res. J. Biol.Sci., **1**(5), pp. 85-90, 2012.

[18] Barud, H.S., Regiani, T., Marques, R.F.C., Lustri, W.R., Messaddeq, Y. & Ribeiro, S.J.L., *Antimicrobial Bacterial Cellulose-Silver Nanoparticles Composite Membranes*, J. Nanomater., **2011**(2011), pp. 1-8, 2011.

[19] Vigneshwaran, N., Nachane, R.P., Balasubramanya, R.H. & Varadarajan, P.V., *A Novel One-Pot 'Green' Synthesis of Stable Silver Nanoparticles using Soluble Starch*, Carbohydr. Res., **341**(12), pp. 2012-2018, 2006.

[20] Kora, A.J., Sashidhar, R.B. & Arunachalam, J., Gum kondagogu *(*Cochlospermum gossypium*): A Template for the Green Synthesis and Stabilization of Silver Nanoparticles with Antibacterial Application*, Carbohydr. Polym., **82**(3), pp. 670-679, 2010.

[21] Kora, A.J., Sashidhar, R.B. & Arunachalam, J., *Aqueous Extract of* Gum olibanum *(Boswelliaserrata): A Reductant and Stabilizer for the Biosynthesis of Antibacterial Silver Nanoparticles*, Process Biochem., **47**(10), pp. 1516-1520, 2012.

[22] van Phu, D., Lang, V.T.K., Lan, N.T.K., Duy N.N., Chau N.D., Du B.D., Cam B.D. & Hien, N.Q., *Synthesis and Antimicrobial Effects of Colloidal Silver Nanoparticles in Chitosan by γ-Irradiation*, J.Exp.Nanosci., **5**(2), pp. 169-179, 2010.

[23] Sharma, S., Sanpui, P., Chattopadhyay, A. & Ghosh, S.S., *Fabrication of Antibacterial Silver Nanoparticle-Sodium Alginate-Chitosan Composite Films*, RSC Adv., **2**(13), pp. 5837-5843, 2012.

[24] Goh, C.H., Heng, P.W.S. & Chan, L.W., *Alginates as a Useful Natural Polymer for Microencapsulation and Therapeutic Applications*, Carbohydr. Polym., **88**(1), pp. 1-12, 2012.

[25] Liu, Y., Chen, S., Zhong, L. & Wu, G., *Preparation of High-Stable Silver Nanoparticle Dispersion by using Sodium Alginate as a Stabilizer under Gamma Radiation*, Radiat. Phys. Chem., **78**(4), pp. 251-255, 2009.

[26] Saha, S., Pal, A., Kundu, S., Basu, S. & Pal, T., *Photochemical Green Synthesis of Calcium-Alginate-Stabilized Ag and Au Nanoparticles and their Catalytic Application To 4-Nitrophenol Reduction*, Langmuir, **26**(4), pp. 2885-2893, 2010.

[27] Chen, P., Zhang, X., Miao, Z., Han, B., An, G. & Liu, Z., *In-situ Synthesis of Noble Metal Nanoparticles in Alginate Solution and their Application in Catalysis*, J. Nanosci. Nanotechnol., **9**(4), pp. 2628-2633, 2009.

[28] Xia, L., Wang, H., Wang, J., Gong, K., Jia, Y., Zhang, H. & Sun, M., *Microwave-Assisted Synthesis of Sensitive Silver Substrate for Surface-Enhanced Raman Scattering Spectroscopy*, J. Chem. Phys., **129**(13), pp. 1-7, 2008.

[29] Hu, B., Wang, S.-B, Wang, K., Zhang, M. & Yu, S.-H., *Microwave-Assisted Rapid Facile "Green" Synthesis of Uniform Silver Nanoparticles: Self-Assembly into Multilayered Films and Their Optical Properties*, J. Phys. Chem. C, **112**(30), pp. 11169-11174, 2008.

[30] Hu, J.-Q., Chen, Q., Xie, Z.-X., Han, G.-B., Wang, R.-H., Ren, B., Zhang, Y., Yan, Z.-L. & Tian, Z.-Q., *A Simple and Effective Route for the Synthesis of Crystalline Silver Nanorods and Nanowires*, Adv. Funct. Mater., **14**(2), pp. 183-189, 2004.

[31] Tsutsui, Y., Hayakawa, T., Kawamura, G. & Nogami,M., *Tuned Longitudinal Surface Plasmon Resonance and Third-Order Nonlinear Optical Properties of Gold Nanorods*, Nanotechnology, **22**(27) July 2011, doi:10.1088/0957-4484/22/27/275203.

[32] Wang, W., Chen, Q., Jiang, C., Yang, D., Liu, X. & Xu, S., *One-step Synthesis of Biocompatible Gold Nanoparticles using Gallic Acid in the Presence of Poly-(N-vinyl-2-pyrrolidone)*, Colloids and Surfaces A: Physicochem. Eng. Aspects, **301**(1-3), pp. 73-79, 2007.

[33] Anh, N.T., Phu, D.V., Duy, N.N., Du, B.D. & Hien, N. Q., *Synthesis of Alginate Stabilized Gold Nanoparticles by γ-Irradiation with Controllable Size Using Different* Au^{3+} *Concentration and Seed Particles Enlargement*, Radiat. Phys. Chem., **79**, pp. 405-408, 2010.

[34] Jovanović, Ž.,Radosavljević, A., Šiljegović, M., Bibić, N., Mišković-Stanković, V. & Kačarević-Popović, Z., *Structural and Optical Characteristics of Silver/Poly(N-vinyl-2-pyrrolidone) Nano Systems Synthesized by γ-irradiation*, Radiat.Phys.Chem., **81**(11), pp. 1720-1728, 2012.

[35] Garcia, M.A., de la Venta, J., Crespo, P., Lopis, J., Penadés, S., Fernández, A. & Hernando, A., *Surface Plasmon Resonance of Capped Au Nanoparticles*, Phys. Rev. B, **72**(24), pp. 1-4, 2005.

[36] Amaladhas, T.P., Sivagami, S., Devi, T.A., Ananthi, N. & Velamma, S.P., *Biogenic Synthesis of Silver Nanoparticles by Leaf Extract of* Cassia angustifolia, Adv. Nat. Sci.: Nanosci. Nanotechnol.,**3**(4), pp. 1-7, 2012.

[37] Sondi, I., Goia, D.V. & Matijević, E., *Preparation of Highly Concentrated Stable Dispersions of Uniform Silver Nanoparticles*, J. Colloid Interface Sci., **260**(1), pp. 75-81, 2003.

[38] Tripathy, A., Raichur, A.M., Chandrasekaran, N., Prathna, T. C. & Mukherjee, A., *Process Variables in Biomimetic Synthesis of Silver Nanoparticles by Aqueous Extract of* Azadirachta indica *(Neem) Leaves*, J. Nanopart. Res., **12** (1), pp. 237-246, January 2010.

[39] Rao, Y.N., Banarjee, D., Datta, A., Das, S.K., Guin, R. & Saha, A., *Gamma Irradiation Route to Synthesis of Highly Re-Dispersible Natural Polymer Capped Silver Nanoparticles*, Radiat. Phys. Chem., **79** (12),pp. 1240-1246, December 2010.

[40] Park, J.Y., Patel, D., Choi, E.S., Baek, M.J., Chang, Y., Kim, T.J.& Lee, G.H., *Salt Effects On the Physical Properties of Magnetite Nanoparticles Synthesized at Different NaCl Concentrations*, Colloids Surf. A: Physicochem. Eng. Aspects, **367** (1-3), pp. 41-46, September 2010.

[41] Jiang, J., Oberdörster, G., Biswas, P., *Characterization of Size, Surface Charge, and Agglomeration State of Nanoparticle Dispersions for Toxicological Studies*, J.Nanopart. Res., **11**(4), pp. 77-89, May 2009.